# Humanlike ankle-foot complex for a biped robot

Kenichi Narioka, Toshiyuki Homma, Koh Hosoda

***Abstract*—In this paper, we propose a design of a robotic ankle-foot complex based on the human functional-anatomic ankle-foot structure. The proposed foot consists of three links, two joints, and four plantar muscles, whose mechanical stiffness can be controlled by utilizing McKibben pneumatic actuators. With this structure, a deformable medial longitudinal arch in a human foot can be emulated. We developed a musculoskeletal biped robot to which the proposed feet are implemented and measured its walking motion, especially the deformation of the robot foot. It is found that the foot generates a truss mechanism and a windlass mechanism, which are important functions of a human foot for shock absorption and energy storage and reuse. We also conducted a walking experiment with various parameters of a plantar muscle's tonus to see how the tonus affects to ground reaction forces (GRFs) and its walking behavior. It is found that the GRF had two peaks as well as human walking and the shape of the GRF curve changes according to the tonus of the plantar muscle. We analyzed the impulse of GRF, finding out that a truss mechanism and a windlass mechanism works effectively with appropriate tonus of the plantar aponeurosis.**

## I. Introduction

An ankle-foot complex is one of the most important region of a human body in bipedal locomotion such as walking because it is a unique one that physically interacts with the environment. Some remarkable functions of a human foot are generated based on the extremely complicated structure including 26 bones, many mono, multi articular muscles, tendons, and other soft tissues [10]. For example, impact absorption and pushing off by a toe are provided by so-called a truss mechanism and a windlass mechanism, which are explained in detail in the following section, lead by the deformation of medial longitudinal arch of the support foot [12], [11].

By contrast, robotic feet of existing humanoids such as [2], [1], [3] tend to be very simple, e.g. flat planes, comparing to a human foot. The reason why these robots wear so simplified feet is supposed to be not only manufactural cost but also control cost due to the lack of compliance of electric motors they use. In other words, humanlike foot mechanisms can be realized if a structure and compliance of a robotic ankle-foot complex are well designed. Then, it is useful to reconsider the robotic foot design, referring to the complicated and compliant human foot in order to improve the performance of bipedal locomotion of humanoid robots.

This work was supported by KAKENHI 23220004 and KAKENHI 24000012.

Kenichi Narioka and Koh Hosoda are with the Department of Multimedia Engineering, Graduate School of Information Science and Technology, Osaka University, 2-1 Yamadaoka, Suita, Osaka, 565-0871, Japan. Toshiyuki Homma is with System Technology Development Center, Corporate Technology Division, Kawasaki Heavy Industries, LTD., 1-1, Kawasaki-cho, Akashi, Hyogo, 673-8666, Japan.)
narioka@ist.osaka-u.ac.jp

Davis and Caldwell [23] developed a well-designed robotic foot that replicates a human foot skeletal structure. Their foot uses springs at the joints and a soft material as a substitute for flesh, realizing the function of adaptability to contours of ground, impacts absorption, and storage and release of energy. However, their model does not have any bi-articular muscle and tendon, which is supposed to be important structure of human musculoskeletal system. In addition, the experiment was conducted using the foot itself without considering wholebody dynamics. It was not discussed how the compliance affects the foot's functions in the context of biped walking. Owaki et al. [21] proposed a biped walker with multi-linked deformable feet whose joints are compliant due to torsion springs. But their model also does not have any bi-articular muscle and tendon. Hashimoto et al.[22] developed a robotic foot that consists of the external toe, the internal toe, and the foot arch joints for their humanoid robot WABIAN-2R. Their foot used a wire as a bi-articular plantar aponeurosis, the structure of which is similar to that of human, and realized the shock absorbing function (truss mechanism) and the push-off function (windlass mechanism) while walking. However, It is still unclear how compliance of the plantar aponeurosis affects the functions and walking behavior.

In this study, we aim to develop a novel robotic ankle-foot complex which has a humanlike deformable arch and can generate the humanlike truss and windlass mechanisms. Our previous studies on limit cycle walkers [4], [5], [6], whose body are based on passivity based walkers [13], [14], [15], [16], focused on the musculoskeletal system which enables the robots to walk without complicated control since the stable behavior can be generated through the interaction between the compliant body and the environment. This paper follows the same line, extending this strategy into foot design. Referring to a human foot, we design a foot with multi links, multi joints, and multi plantar muscles, utilizing pneumatic actuators that can have variable compliance. The first goal of this study is to design the robotic foot and to verify that it can generate the truss and windlass mechanisms. The second one is to investigate the effect of compliance of the plantar aponeurosis on the walking behavior.

The contents of this paper are as follows. First, we introduce the biped robot including ankle-foot design in section 2. Second, we analyze the foot motion while walking to verify the truss and windlass mechanisms occur in section 3. In the section, we also discuss the effect of tonus of the plantar muscles. Finally, we conclude this paper in section 4.

## II. Robot Design

### A. System overview

We have designed and built a biped robot named "Pneumat-BB", the appearance of which is shown in Fig.1. This robot has a body length of around 1100 mm and a weight of around 11.0 kg. Magnesium alloy and acrylonitrile butadiene styrene are used as structural material. The robot has totally 10 DOF, including hip, knee, ankle, and two joints in a foot, which will be explained in detail in the following subsection, for one leg. All joints of the robot are driven by McKibben pneumatic artificial muscles [8], [9], [7], that consists of an inner rubber tube and an outer nylon sleeve. As shown in Fig. 2, it contracts when compressed air is supplied to the inner tube. Its contraction ratio depends on its inner pressure while its maximum contraction ratio is around 25%. The stiffness of the pneumatic muscle is also changed according to the inner pressure. The configuration of the pneumatic muscles of the robot shown in Fig. 3 refers to human musculoskeletal structure. There are six mono-articular muscles; iliacus (hip flexor), gluteus maximus (hip extensor), vastus medialis (knee extensor), popliteus (knee flexor), tibialis anterior (ankle dorsal flexor), and soleus (ankle plantar flexor). In addition, there are three bi-articular muscles; rectus femoris (hip flexor and knee extensor), hamstring muscles (hip extensor and knee flexor), and gastrocnemius (knee flexor and ankle plantar flexor).

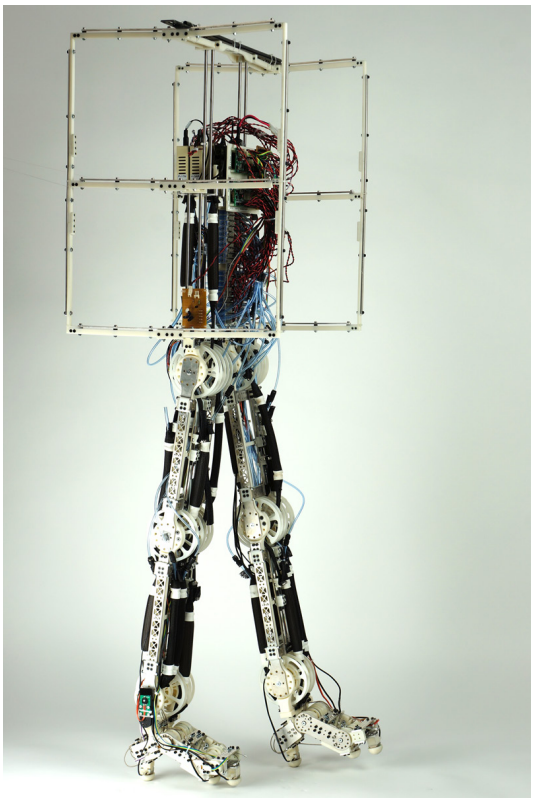

Fig. 1. Biped robot "Pneumat-BB".

Pneumatic and electric signal flow is shown in Fig. 4.

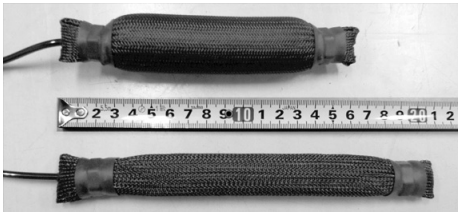

Fig. 2. McKibben pneumatic muscle. Compressed air is supplied (top). The air is exhausted (bottom) .

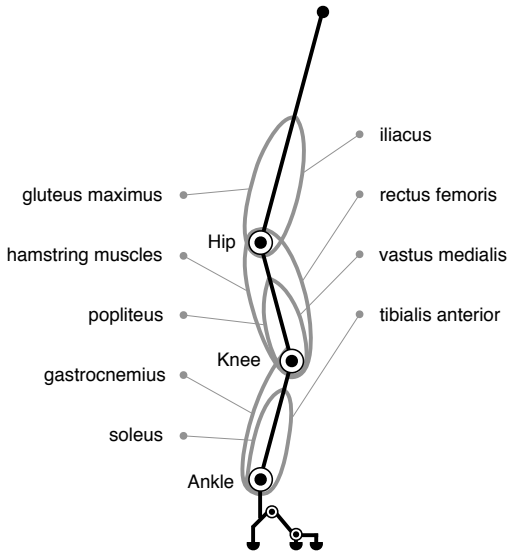


Fig. 3. Musculoskeletal structure of Pneumat-BB.

The robot contains micro control boards, a Li-po battery, and on/off solenoid valves within its body. Compressed air is supplied to the valves from an external compressor via an air regulator. Joint angles, GRFs, and inner pressures of pneumatic muscles are measured by potentiometers at joints of feet, load cells on the feet, and pressure sensors attached to the plantar pneumatic muscles, respectively. The sensory information is sent to the micro controller via A/D converter and then can be monitored in PC using serial communication.

### B. Humanlike foot design

A human foot has a structure based on three arches; medial longitudinal arch, lateral longitudinal arch, and transverse arch. We focus on the medial longitudinal arch (hereafter "arch") since it is known as very important part in supporting and propelling the body while locomotion. The way of deformation and its function in a walking cycle is illustrated in Fig. 5. The arch can be thought of as a truss that consists of two sides of bone and base of plantar aponeurosis. After heel strike of stance foot (a), arch gets lower since the body press the truss (b). While this truss mechanism absorbs impact, the plantar aponeurosis is extended. Toe joint get extended after heel off, so that the arch get higher again due to the contraction of the plantar aponeurosis (c). This is called a windlass mechanism, which enables effective pushing off of

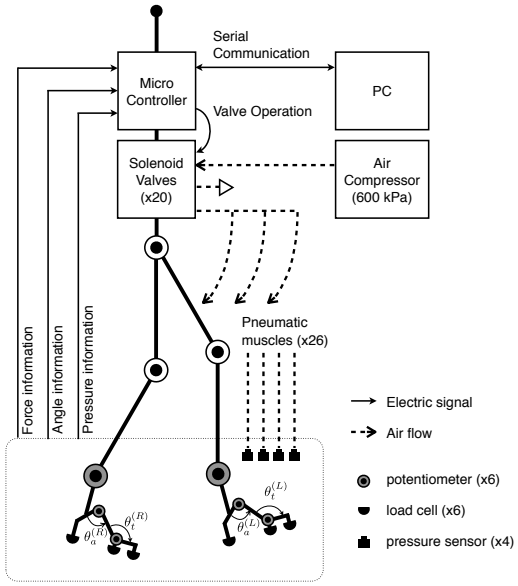


Fig. 4. Pneumatic and electric system of Pneumat-BB

the toe until toe off (d). The plantar aponeurosis relates to both mechanisms and plays a key role. In other words, the plantar aponeurosis accumulates the energy in the former term (b) and release it in the latter term (c) in a reasonable way.

A human foot can be roughly divided into a fore foot, a mid foot, and a hind foot from a functional point of view. Based on this division, we design a foot with three links and two joints as shown in the left side of Fig.6. The height of the arch is determined by the joint A, which corresponds to talus, navicular, cuboid, and cuneiform complex of a human foot. The joint T corresponds to MP joint of a human foot. Four pneumatic muscles, which correspond to extensor digitorum brevis, flexor hallucis brevis, long plantar ligament, and plantar aponeurosis are arranged as shown in the right side of Fig.6. The CAD design and the actual equipment are shown in Fig.7. A pressure sensor is implemented to the plantar aponeurosis to control its tonus in the following experiments. Load cells are on the hind foot, the mid foot, and the fore foot to detect the heel strike and also to measure GRF while walking. An external force plate can be used in the experiment as a matter of practical convenience.

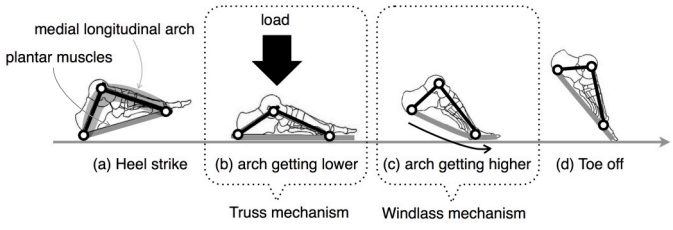


Fig. 5. Deformation of stance foot and related mechanisms

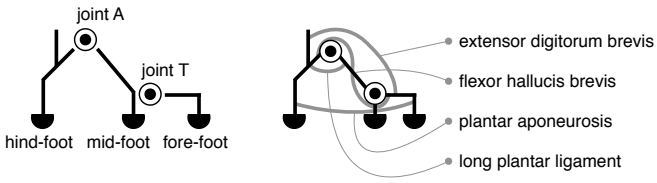


Fig. 6. Ankle-foot structure and muscle arrangement

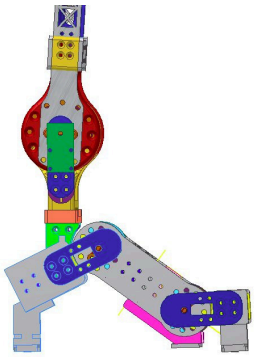

(a) CAD design

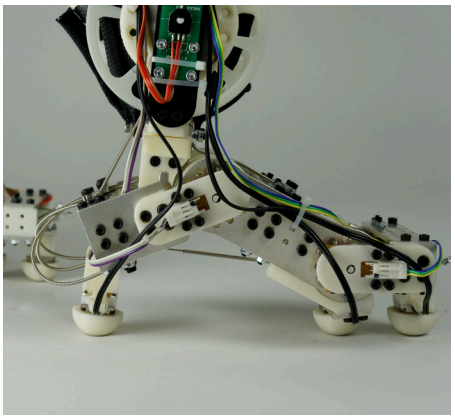

(b) Actual equipment

Fig. 7. Foot design and actual equipment

## III. Analysis of Walking

### A. Walking controller

The robot is driven by a simple open-loop controller, which is basically same as that of our existing biped robot [6]. The controller gives a certain activation pattern to each muscle within one walking cycle, which is triggered by a heel strike. The valve operation patterns of muscles are illustrated in Fig. 8, while its parameters are shown in Table I.

- A certain amount of air is supplied to iliacus, rectus femoris, hamstring muscles, gastrocnemius, extensor digitorum brevis, flexor hallucis brevis, and long plantar ligament only before a walking trial and kept that amount through the walking trial. Compressed air is not supplied to popliteus, so that inner pressure of the

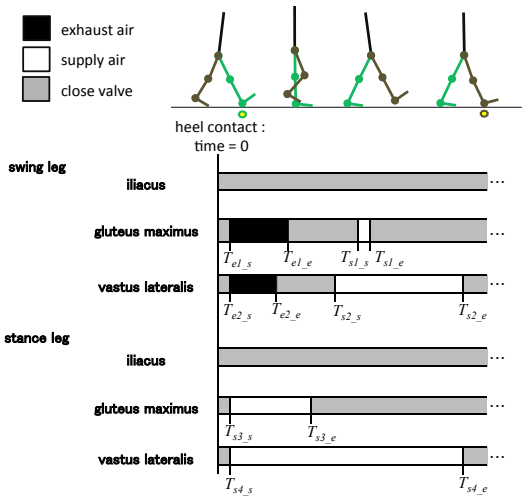


Fig. 8. Walking controller

muscle is always the same as atmospheric pressure. That is, popliteus plays no role in the experiment in this paper.

- The air is exhausted from gluteus maximus of swing leg and supplied to gluteus maximus of stance leg in the early period of a walking cycle, from $T_{e1\_s}$ to $T_{e1\_e}$. These operations flex the hip joint of the swing leg and extend the hip joint of stance leg, respectively. The air is also supplied to gluteus maximus of swing leg in the latter period of the cycle, which makes a retraction motion.
- The air is exhausted from vastus medialis, which makes the knee joint free so that the swing knee flexes naturally with the hip swinging motion and the swing foot can pass the ground around midstance. After that, the air is supplied to vastus medialis to extend the knee. The knee joint has a patella structure that prevents the hyperextension of the joint.
- Inner pressure of the plantar aponeurosis is controlled to be $P_{\mathrm{PA}}$ before a walking trial and kept that amount through the trial. Those are control parameters in the following experiments.

### B. Kinematic analysis

In this part, we demonstrate the walking behavior of the robot and analyze it from kinematic perspective in order to evaluate the developed foot. The robot walks on a treadmill, the velocity of which is fixed to be around 0.25 m/s. The sideways motion of the robot is constrained by the iron steel bars so that the robot does not have to care about its lateral balance. Note that the restraint affects sagittal motion negligibly since the friction between ABS and steel bar is very small.

We found that the robot can walk stably with certain pressure of the plantar aponeurosis $P_{\mathrm{PA}}$ . As an example, a walking movement of the robot with $P_{\mathrm{PA}}$=450 kPa is shown in Fig. 9. Then we measured the angle of the joint A and T while walking. The result is shown in Fig. 10, where $\theta_a, \theta_t$ of right foot are plotted. Here, time 0 in the graph indicates the timing of heel strike of right foot. We found that the arch of the stance foot get lower in the mid-term of a walking cycle. By contrast, the arch get higher and the joint T extended in the late-term. This result indicates that both truss mechanism and windlass mechanism works well.

TABLE I
PARAMETER OF WALKING CONTROLLER

| Function | | | | Parameter | Value [ms] |
|---|---|---|---|---|---|
| Stance leg | hip | flexion | start | $T_{e1\_s}$ | 0 |
| | | | end | $T_{e1\_e}$ | 230 |
| | | extension | start | $T_{s1\_s}$ | 550 |
| | | | end | $T_{s1\_e}$ | 600 |
| | knee | flexion | start | $T_{e2\_s}$ | 0 |
| | | | end | $T_{e2\_e}$ | 200 |
| | | extension | start | $T_{s2\_s}$ | 450 |
| | | | end | $T_{s2\_e}$ | 1000 |
| Swing leg | hip | extension | start | $T_{s3\_s}$ | 0 |
| | | | end | $T_{s3\_e}$ | 350 |
| | knee | extension | start | $T_{s4\_s}$ | 0 |
| | | | end | $T_{s4\_e}$ | 1000 |

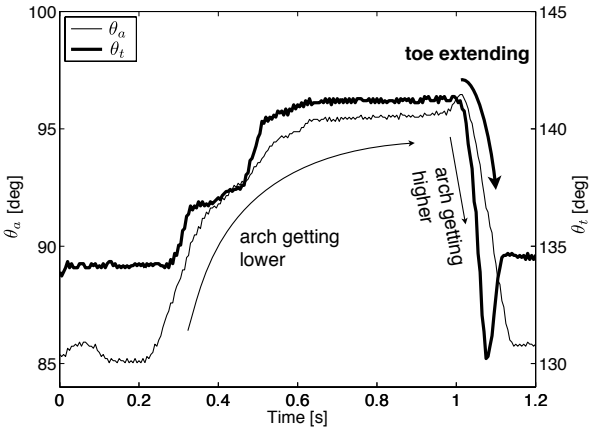


Fig. 10. Deformation of the joint A and the joint T within a walking cycle.

### C. GRF analysis

We measured vertical GRF of a step using a force plate (Tech Gihan Co., Ltd., TF-3040) with various values of parameters of $P_{\mathrm{PA}}$: 250, 350, 450, and 550 kPa. In addition to these four conditions, the joint A and T were mechanically fixed with metal plates as a control condition. Since the robot could not walk stably by itself with some conditions, experimenter supported the robot's motion from backward slightly. Fig. 11 shows the result with three trials in each condition. Walking cycle in each condition was around 1 second. We found that GRF becomes higher in early-term (0-0.2 s) and in late-term (0.6-1.0 s), while get lower in mid term (0.2-0.6 s). This twin peaks of GRF is well known as the characteristics of human walking. In order to see the effect of the plantar aponeurosis more quantitatively, we calculate

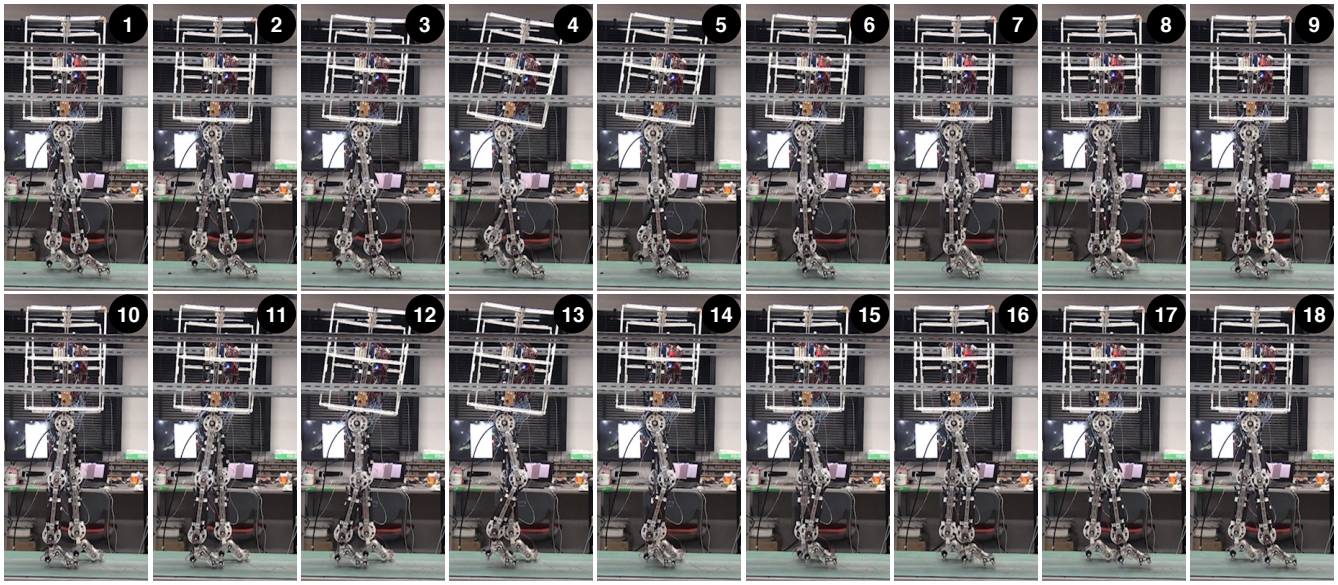


Fig. 9. Walking behavior of Pneumat-BB.

impulse in each term. The result is shown in Fig. 12. The impulse in mid-term gets smaller as the inner pressure of the plantar aponeurosis decreases. The lower impulse indicates that the truss mechanism reduces the impact of the ground contact.

On the other hand, impulse in late-term gets maximum when $P_{\mathrm{PA}}$=450 kPa. The higher impulse indicates that the windlass mechanism increases the pushing off by the toe. The reason why the impulse has non-linear curve can be considered as following. When the compliance of the plantar aponeurosis is low, restoring force becomes relatively small. On the contrary, when the compliance of the plantar aponeurosis is high, range of extension becomes relatively small. So, there is well balanced compliance of the plantar aponeurosis for the truss mechanism and the windlass mechanism.

## IV. Conclusion

In this study, we proposed a novel robotic ankle-foot complex that consists of three links and plantar muscles using McKibben pneumatic actuators. The foot design is based on human functional-anatomic foot structure.

First, we implemented the foot to our musculoskeletal biped robot and confirmed that the biped can walk stably with the certain compliance of the plantar muscles utilizing the existing controller we have proposed previously. Second, we measured the angles of foot joints while walking. Getting lower of the arch in the mid-term of the walking cycle indicates the generation of the truss mechanism. By contrast, getting higher of the arch and the extension of MP joint of stance foot in the late-term indicates the generation of the windlass mechanism. Third, we measured the GRFs with various conditions of the plantar aponeurosis to see how the tonus affects to walking behavior. We found that GRF has basically two peaks with every parameters, but the shape differs each other. We analyzed the impulse of GRF during a mid-term and a late-term of the support phase and found out that truss mechanism and windlass mechanism emerged with appropriate tonus of the plantar aponeurosis.

In future, we are going to investigate the role of developed foot for walking performance such as velocity, stability, and efficiency. We are also going to investigate the effect of the proposed foot on roll-over shape (ROS), which characterizes the rocker function of human foot. Some interesting result about ROS are reported in studies in biomechanics, such that the ROS maintains a similar circular shape under various conditions such as added weight [17], different heel height of shoes [19], different walking speed [18] and inclined surfaces[20]. It can be a new paradigm for walking robots.

## References

[1] S. Kajita et al. A realtime pattern generator for biped walking. *Proceedings of the 2002 IEEE International Conference on Robotics and Automation (ICRA)*, pp.31-37, 2002.

[2] K. Hirai et al. The development of Honda humanoid robot *Proceedings of the 1998 IEEE International Conference on Robotics and Automation (ICRA)*, pp.1321-1326, 1998.

[3] Y. Ogura et al. Evaluation of various walking patterns of biped humanoid robot. *Proceedings of the 2005 IEEE International Conference on Robotics and Automation (IROS)*, pp.605-610, 2005.

[4] Takashi TAKUMA, Koh HOSODA, and Minoru ASADA. Walking stabilization of biped with pneumatic actuators against terrain changes. *IEEE/RSJ International Conference on Intelligent Robots and Systems*, pp. 2775–2780, 2005.

[5] Koh Hosoda, Kenichi Narioka. Synergistic 3D Limit Cycle Walking of an Anthropomorphic Biped Robot. *IEEE/RSJ International Conference on Intelligent Robots and Systems*, pp. 470–475, 2007.

[6] Kenichi Narioka, Koh Hosoda. Designing Synergistic Walking of a Whole-Body Humanoid driven by Pneumatic Artificial Muscles: An empirical study. *Advanced Robotics*, Vol.22 No.10, pp.1107-1123,2008.

[7] Ryuma Niiyama, Yasuo Kuniyoshi Pneumatic Biped with an Artificial Musculoskeletal System *Proceedings of 4th International Symposium on Adaptive Motion of Animals and Machines, pp.80-81*,2008.

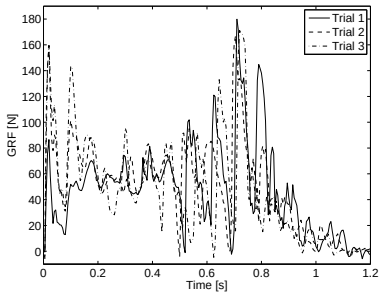


(a) $P_{\mathrm{PA}}$=250 kPa

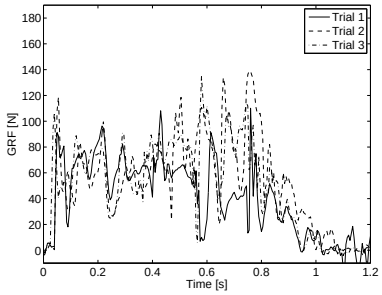


(b) $P_{\mathrm{PA}}$=250 kPa

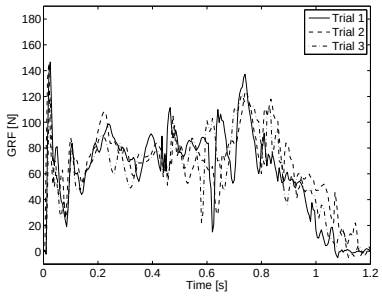


(c) $P_{\mathrm{PA}}$=250 kPa

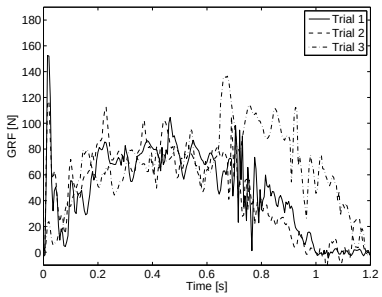


(d) $P_{\mathrm{PA}}$=250 kPa

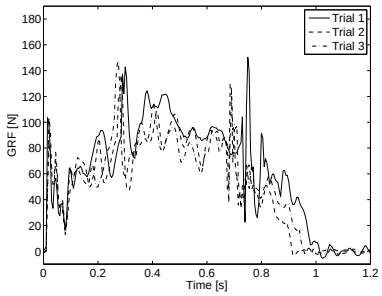


(e) Joint A and T are fixed mechanically.

Fig. 11. GRF within one walking step. Three trials are done for each parameter.

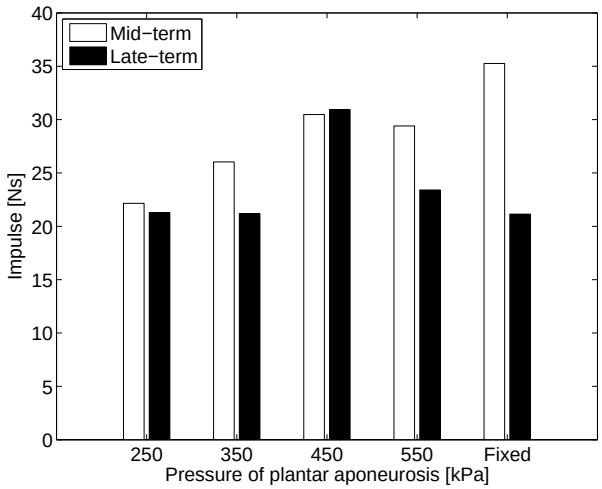


Fig. 12. Impulse of GRF. Mid-term is from 0.2 to 0.6 s. Late-term is from 0.6 to 1.0 s


[8] D. Caldwell et al. Control of pneumatic muscle actuators *IEEE Control Systems, pp.40-47*, 1995.

[9] R. van der Linde, Design, Analysis, and Control of a Low Power Joint for Walking Robots by Phasic Activation of McKibben Muscles *IEEE Transactions on Robotics and Automation, Vol.15, No.4, pp.599-604*, 1999.

[10] M. Schuenke, E. Schulte, U. Schumacher, Thieme Atlas of Anatomy. General Anatomy and Musculoskeletal System. *THIEME*, 2010.

[11] D. Neumann, kinesiology of the musululoskeletal system. *Mosby*, 2002.

[12] I.A. kapandji, physiologie articulaire. *Maloine S.A. éditeur*, 1985.

[13] T.McGeer. Passive dynamic walking. *Int. J. of Robotics Research*, Vol. 9, No. 2, pp. 62–82, 1990.

[14] M.Wisse and J. van Frankenhuyzen. Design and construction of mike; a 2D autonomous biped based on passive dynamic walking. *Proc. of the 2nd International Symposium on Adaptive Motion of Animals and Machines*, 2003.

[15] M.Wisse. Three additions to passive dynamic walking; actuation, an upper body, and 3D stability. *IEEE-RAS/RSJ International Conference on Humanoid Robots*, 2004.

[16] Steven H. Collins, and Andy Ruina. A bipedal walking robot with efficient and human-like gait. *Proc. of the 2005 IEEE Int. Conf. on Robotics and Automation, pp. 1995–2000*, 2005.

[17] A.Hansen, D.Childress, Knox. Effects of adding weight to the torso on roll-over characteristics of walking. *Journal of Rehabilitation Research and Development, Vol.42, No.3, pp.381-390*,2005.

[18] A.Hansen, D.Childress, Knox. Roll-over Shapes of Human Locomotor Systems: Effects of Walking Speed. *Clinical Biomechanics, Vol. 19, No. 4, 407-414*, 2004.

[19] A.Hansen, D.Childress. Effects of Shoe Heel Height on Biologic Roll-over Characteristics During Walking. *Journal of Rehabilitation Research and Development, Vol.41, No.4, 547-554*, 2004

[20] A.Hansen, D.Childress, S.Miff. Roll-over characteristics of human walking on inclined surfaces. *Human Movement Science, Vol.23, Issue 6, pp. 807-821*, 2004

[21] D. Owaki, S. Kubo, A. Ishiguro, A CPG-based Control of Bipeda Locomotion by Exploiting Deformable Feet. *Proc. of the 5th International Symposium on Adaptive Motion of Animals and Machines (AMAM2011)*,pp. 79-80, 2011.

[22] Kenji Hashimoto, Yuki Takezaki, Kentaro Hattori, Hideki Kondo, Takamichi Takashima, Hun-ok Lim, Atsuo Takanishi, A study of function of foot's medial longitudinal arch using biped humanoid robot. *IEEE/RSJ International Conference on Intelligent Robots and Systems*,pp.2206-2211, 2010.

[23] S. Davis, Darwin G. Caldwell, The design of an anthropomorphic dexterous humanoid foot. *IEEE/RSJ International Conference on Intelligent Robots and Systems*,pp.2200-2205, 2010.